DYNAMIC MODELING AND EXPERIMENTAL VALIDATING OF LARGE SEMI-RIGID STRUCTURES

D.-X. Li * W. Liu X.-Y. Sun

College of Aerospace Science and Engineering
National University of Defense and Technology
Changsha, Hunan 410073, P. R. China

ABSTRACT

A new type of large semi-rigid solar array structure with a new structural concept of rigid-flexible combination has developed for space application. Due to the good features of large scale and light-weight, such structure can well satisfy to the large power requirements of spacecraft and thus has drawn increasing attention recently. However, its structural weakness of inherently flexibility makes low frequency vibrations happen much easier. It is highly required to obtain an accurate dynamic model for predicting the dynamic characteristics of this kind of semi-rigid space structure. Because this structure is composed of different components that have quite different stiffness properties respectively, it is very difficult to build up an accurate dynamic model of this complex structure. In this paper, a novel analytical dynamic model is developed for solving this problem. To validate the correctness of the proposed model, experiment studies are conducted. By comparing the simulation results with experimental results, it can be concluded that this dynamic modeling method presented in the paper is credible. The present study is significant for the structural construction and application of this special structure.

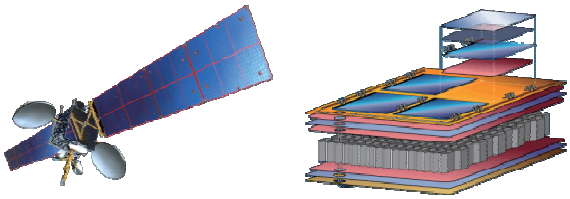
Keywords: Semi-rigid structure, Dynamic model, Membrane-frame, Experiment validating.

1. INTRODUCTION

Nowadays, space solar array structures become larger and lighter due to the energy requirements of spacecraft and the stringent restrictions of launch cost [1]. As a new type of lightweight space structures, large semi-rigid solar array structures (LSSAS) are of continued research interest by many organizations in recent years, and being developed for potential space applications including the power collection and conversion devices of spaceships, space stations, space laboratories, *etc.* [2-4]. This new breed of large semi-rigid space structure embodies a typical structural concept of rigid-flexible combination, and has many superior advantages such as large scale (up to 100m^2) and lightweight (less than 1kg/m^2).

Nevertheless, this type of semi-rigid structure encounters a serious dynamic problem due to its inherent flexibility. It is very easy for this type of semi-rigid structure to be stirred up low frequency vibrations, which will seriously degrade the performance of spacecraft and even disrupt the space missions. Therefore, to obtain an accurate dynamic model for predicting the dynamic behavior of the structure is highly required in engineering.

But, it is very difficult to do so due to the complexity of the structural construction. In contrast to those traditional rigid solar array structures, which usually made of an aluminum honeycomb structure covered with carbon fiber panels on both sides as shown in Fig. 1, a



(a) Rigid solar array (b) Structural construction

Fig. 1 Diagram of a traditional rigid solar array structure [14]

LSSAS is composed of different components, such as solar cells, flexible fiber nets and a perimeter rigid supporting frame. Hence, we view it as a semi-rigid structure here (see Fig. 2). These components have quite different stiffness properties respectively. For instance, the solar cells are of membrane type structural properties, the fiber nets are of string type structural properties, and the perimeter rigid supporting frame are of beam type structural properties.

However, owing to the complicated structural characteristics, it is very difficult to build up an accurate dynamic model for describing the dynamic properties of this type of semi-rigid structures. Until recently, there are few published studies concerning about the dynamic modeling problem of such semi-rigid solar array structures [5-13]. S. W. Smith, *et al.* [5] developed two kinds of beam-type models (a cantilevered beam with a tip mass and a double-T-shaped structure composed of

* Corresponding author (dongxuli@nudt.edu.cn)

DOI : 10.1017/jmech.2014.5
Copyright © 2014 The Society of Theoretical and Applied Mechanics, R.O.C.
https://doi.org/10.1017/jmech.2014.5 Published online by Cambridge University Press

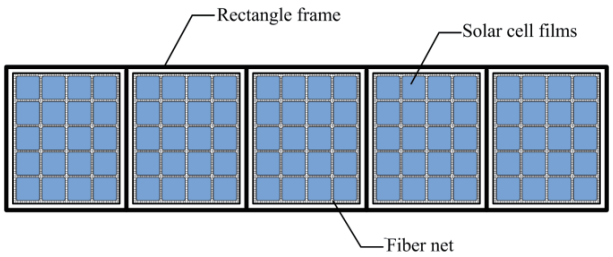


Fig. 2 Schematic of a large semi-rigid solar array structure

six beams) to analyze nonlinear planar responses of a semi-rigid laboratory solar array. Kyung-Eun Ko, *et al.* [6] employed a thin-walled composite beam model to conduct the coupled thermal-structural analysis of solar arrays. K. S. Carney, *et al.* [7] established a cantilevered plate model of a space station solar array by applying the equations of continuum mechanics. All these above studies used the relative simple beam/plate models, and did not take the influence of solar cell film stiffness on the system dynamic performance into account.

In this paper, an innovative analytical model, which we name it as membrane-frame model, is developed for the dynamic analysis of this semi-rigid solar array structure. Experimental studies, including stiffness measurement of a solar cell and modal test of the semi-rigid solar array structure, are conducted for the purpose of parameter measuring and dynamic model validating. By comparing the numerical simulation results with the experimental results, it can be concluded that the modeling and experiment methods presented in this paper are credible and usable for structural dynamic characteristic predicting and vibration control design of this new type of semi-rigid structures.

2. DYNAMIC MODELING

Referring to Fig. 2, a semi-rigid solar array structure mainly consists of three components: A rigid rectangle frame, a flexible fiber net, and many of thin solar cell films. The rectangle frame is a stiff perimeter supporting structure having high dimensional stability. The fiber net is formed by dense interconnected quadrangles, which are generated through the way that threadlike fibers extend across the rectangle frame surface. The solar cells, acting as the solar power collection and conversion devices, are attached to the surface of the fiber net.

In the dynamic modeling of this special type of semi-rigid structures, how to deal with the influence of the solar cell film stiffness on the system dynamic characteristics is very important. In this paper, according to the relative value between the equivalent stiffness of the solar cell film and that of the fiber net, a simplified model called membrane-frame model is established for the dynamic analysis of a LSSAS. The modeling process will be discussed in detail as below.

Because the bending stiffness of the solar cell film is very small, the combined structure of fiber net and solar cells can be simplified as a membrane model. However, the frame can be simplified as rigid frame model due to the bending stiffness of the frame is quite strong. Thus, the solar array structure can be simplified as a membrane-frame model. In this model, the membrane is pretensioned and coupled to the rigid frame. Therefore, the proposed model can be described as a pretensioned membrane surrounded by a rectangular rigid frame consisting of four beams, as illustrated in Fig. 3. Next, we establish the specific mathematical equations for this model.

2.1 Equations of Motion for the Membrane

A membrane is basically a two dimensional system that lies in a plane when in equilibrium. The structure itself provides no resistance to bending, so that the restoring force is only due to the tension in the membrane. Let $W(x, y, t)$ represent the displacement in the z direction of a membrane lying in the x-y plane at the point (x, y) and the time t, as shown in Fig. 4.

The equations of motion for the membrane is given by [15]

$$\rho \frac{\partial^2 W}{\partial t^2} = T\left(\frac{\partial^2 W}{\partial x^2} + \frac{\partial^2 W}{\partial y^2}\right) + p, \quad x, y \in \Omega \tag{1}$$

where p is the external force exerted on the membrane; Ω denotes the region in the x-y plane occupied by the membrane; T is the tensile force per unit length of the membrane, which is assumed the same in all directions; ρ is the mass per unit area of the membrane.

Considering the special case of no external loading in this study, Eq. (1) can be rewritten as

$$\nabla^2 W - \left(\frac{\rho}{T}\right)\frac{\partial^2 W}{\partial t^2} = 0, \quad x, y \in \Omega \tag{2}$$

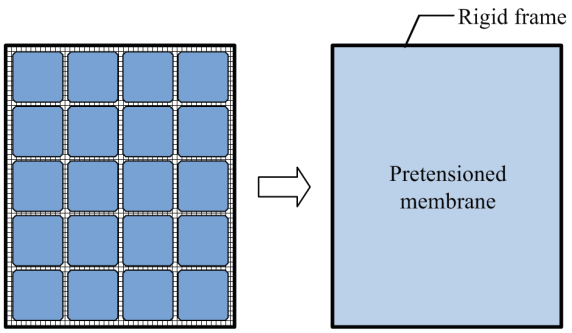
where $\nabla^2 = \dfrac{\partial^2}{\partial x^2} + \dfrac{\partial^2}{\partial y^2}$ is the two-dimension Laplace operator.

2.2 Equations of Motion for the Frame

In this membrane-frame model, the shape of the boundary is a rigid frame structure. Here, "rigid" is relative to the inner flexible fiber net. Actually, it is flexible, and we shall treat the rigid frame as four flexible beam columns in the study. Considering the boundary supporting frame is compressed due to the tension in the membrane, the equations of motion for the frame can be described by [16]

$$\begin{cases} EI_y \dfrac{\mathrm{d}^4}{\mathrm{d}x^4} X(x,t) + \dfrac{1}{2} BT \dfrac{\mathrm{d}^2}{\mathrm{d}x^2} X(x,t) + \rho_b \dfrac{\mathrm{d}^2}{\mathrm{d}t^2} X(x,t) = 0, \\ \qquad\qquad\qquad\qquad\qquad\qquad\qquad\qquad\qquad\qquad y = \pm\dfrac{A}{2} \\ EI_x \dfrac{\mathrm{d}^4}{\mathrm{d}y^4} Y(y,t) + \dfrac{1}{2} AT \dfrac{\mathrm{d}^2}{\mathrm{d}y^2} Y(y,t) + \rho_b \dfrac{\mathrm{d}^2}{\mathrm{d}t^2} Y(y,t) = 0, \\ \qquad\qquad\qquad\qquad\qquad\qquad\qquad\qquad\qquad\qquad x = \pm\dfrac{B}{2} \end{cases} \tag{3}$$

https://doi.org/10.1017/jmech.2014.5 Published online by Cambridge University Press



(a) Physical model (b) Simplified model

Fig. 3 Schematic of the membrane-frame model

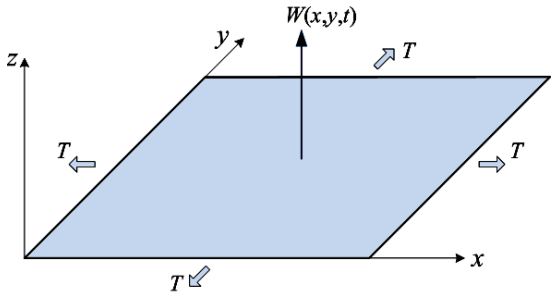


Fig. 4 A pretensioned membrane element

where A, B are the length and width of the frame, respectively; X, Y are the transverse displacements of the supporting frame in the z direction; Ix, Iy are the cross sectional moments of inertia about x, y axis's, respectively; E and ρ_b are the elastic modulus and mass per unit length of the supporting beam.

As mentioned above, there are no external force and moment acting on the frame. Thus, Eq. (3) has the following free-free-free-free boundary conditions

$$\begin{cases} \left.\dfrac{\mathrm{d}^2X(y,t)}{\mathrm{d}y^2}\right|_{y=\pm\frac{A}{2}} = \left.\dfrac{\mathrm{d}^4X(y,t)}{\mathrm{d}y^4}\right|_{y=\pm\frac{A}{2}} = 0\,, \quad x=\pm\dfrac{B}{2} \\ \left.\dfrac{\mathrm{d}^2Y(x,t)}{\mathrm{d}x^2}\right|_{x=\pm\frac{B}{2}} = \left.\dfrac{\mathrm{d}^4Y(x,t)}{\mathrm{d}x^4}\right|_{x=\pm\frac{B}{2}} = 0\,, \quad y=\pm\dfrac{A}{2} \end{cases} \tag{4}$$

where $d^2(\ ) = 0$ denotes the boundary condition of moment balance, while $d^4(\ ) = 0$ denotes the boundary condition of force equilibrium.

Substituting the above boundary conditions (4) into Eq. (3), we can obtain the solution of Eq. (3) in the following form

$$\begin{cases} X(y,t) = \left[a_1\sin(k_1y) + a_2\cos(k_1y) + a_3\sinh(k_2y) \right. \\ \qquad \left. + a_4\cosh(k_2y)\right]\sin(\omega_{b1}t+\varphi_1)\,, \quad x=\pm\dfrac{B}{2} \\ Y(x,t) = \left[b_1\sin(p_1x) + b_2\cos(p_1x) + b_3\sinh(p_2x) \right. \\ \qquad \left. + b_4\cosh(p_2x)\right]\sin(\omega_{b2}t+\varphi_2)\,, \quad y=\pm\dfrac{A}{2} \end{cases} \tag{5}$$

where

$$\begin{cases} k_{1,2} = \sqrt{\mp\dfrac{BTA^2}{4EI_y} + \dfrac{1}{2}\sqrt{\left(\dfrac{BTA^2}{2EI_y}\right)^2 + \dfrac{4\rho_bTA^2}{\rho EI_y}\omega_{b1}^2}} \\ p_{1,2} = \sqrt{\mp\dfrac{ATB^2}{4EI_x} + \dfrac{1}{2}\sqrt{\left(\dfrac{ATB^2}{2EI_x}\right)^2 + \dfrac{4\rho_bTB^2}{\rho EI_x}\omega_{b2}^2}} \end{cases} \tag{6}$$

Herein ω_{b1} and ω_{b2} are the natural frequencies of the beams in the x, y directions, respectively.

2.3 General Equations for the Membrane-Frame Structure

To acquire the solution of Eq. (2), the boundary conditions of the membrane should be specified. Here, we treat the frame as the boundary conditions of the membrane.

By applying the displacement-continuity conditions, we have

$$\begin{cases} W\left(\pm\dfrac{A}{2}, y, t\right) = X(y,t)\Big|_{y\in\left[-\frac{B}{2},\frac{B}{2}\right]} \\ W\left(x, \pm\dfrac{B}{2}, t\right) = Y(x,t)\Big|_{x\in\left[-\frac{A}{2},\frac{A}{2}\right]} \end{cases}, \tag{7}$$

By using the moment-equilibrium conditions, we obtain

$$\begin{cases} M\left(\pm\dfrac{A}{2}, y, t\right) = EI_x\dfrac{\mathrm{d}^2}{\mathrm{d}y^2}Y(y,t)\Big|_{y\in\left[-\frac{B}{2},\frac{B}{2}\right]} \\ M\left(x, \pm\dfrac{B}{2}, t\right) = EI_y\dfrac{\mathrm{d}^2}{\mathrm{d}x^2}X(x,t)\Big|_{x\in\left[-\frac{A}{2},\frac{A}{2}\right]} \end{cases}. \tag{8}$$

Thus, we can derive the general equations of motion for the membrane-frame structure by combining Eqs. (2), (5), (7) and (8).

2.4 Numerical Simulation

To demonstrate the correctness and rationality of the above proposed dynamic model, modal analyses of a LSSAS are conducted by numerical simulation. The parameters of LSSAS used for analysis are as follows:

- Dimensions of the solar array: 4800 × 600 × 15mm
- Dimensions of the solar cell film: 40 × 40 × 0.3mm
- Bending stiffness of the fibre net: 220GPa
- Tensile force in the fibre net: 5N
- Mass density of the fibre net: 15kg/m^3
- Bending stiffness of the solar cell film: 22GPa
- Mass density of the solar cell film: 25kg/m^3
- Elastic modulus of the supporting beam: 170GPa
- Mass per unit length of the supporting beam: 1200kg/m^3
- Shape of cross section of the supporting beam: Square
- Cross sectional dimensions of the supporting beam: 12 × 12mm

https://doi.org/10.1017/jmech.2014.5 Published online by Cambridge University Press

Based on the dynamic model established, the natural frequencies and mode shapes are calculated. The first five mode shapes of the membrane-frame model are shown in Fig. 5, and the first five natural frequencies of the model are listed in Table 1. At the same time, numerical simulation of the modal characteristics of the LSSAS is conducted by using the FEM software package (the NASTRAN is used in the study), and the computed results of the natural frequencies is also listed in Table 1. We can conclude from this table that the analytical solutions agree well with the FEM solution.

3. EXPERIMENT STUDIES

In this section, experiment studies regarding to a LSSAS are conducted. First, the stiffness of the solar cell film is measured to determine whether the simplified model is appropriate for the solar array. Then, to verify the validity and accuracy of the proposed dynamic model, a modal analysis experiment of the solar array is carried out.

3.1 Solar Cell Film Stiffness Measurement

In this study, we present a novel experimental method to measure the solar cell film stiffness, as illustrated in Fig. 6.

This experimental testing method is a noncontact photogrammetry measurement method based on a three-point bending principle. First, we put the solar cell film need to be tested on two parallel supporters. Then, the solar cell film is loaded via the way of adding standard weights step by step to a hanger, which is hanged on the middle of the solar cell film. Finally, every bending deformation caused by the standard weights is measured through image processing techniques. The structural and material parameters of the solar cell film used for test are same as those mentioned in Section 2.4. The testing result is plotted with a load-deflection curve, as shown in Fig. 7.

From Fig. 7, it can be found that the relationship between the deflection and the mass of the standard weights is nonlinear. This is because the elastic modulus of the solar cell film is not constant since the solar film is formed by stacking multi-layer different materials.

Based on the three-point bending formula [17], the equivalent bending stiffness of the solar cell film can be calculated by

$$E_f = \frac{a^3 \Delta p}{4bh^3 \Delta f} \tag{9}$$

where Δp is the load increment on the load-deflection curve, Δf is the corresponding deflection increment with regard to Δp.

By applying Eq. (9), we can get that the equivalent bending stiffness of the tested solar cell film is 20.416GPa from Fig. 7. Compared with the given value of the fiber net stiffness (220GPa), we find that the measured stiffness of the solar cell film is less than 1/10 of that of fiber net, thus the stiffness of fiber net is dominating in the membrane model.

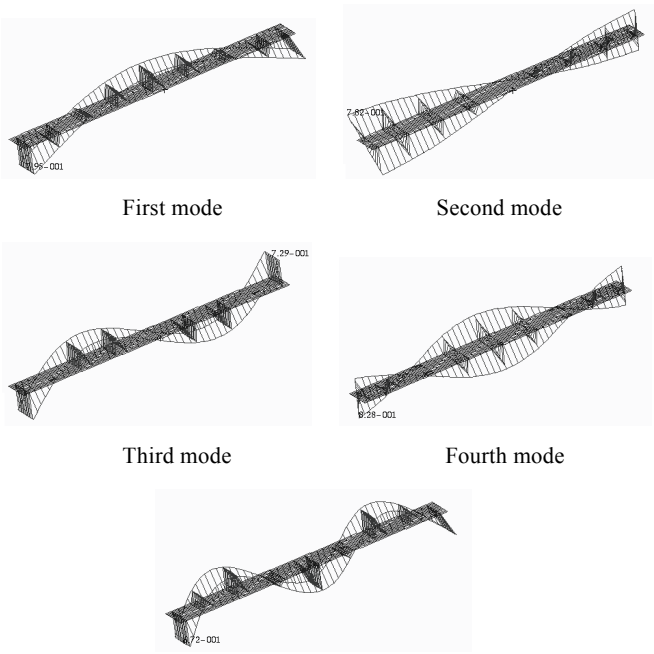


Fig. 5 Mode shapes for a LSSAS with the proposed dynamic model

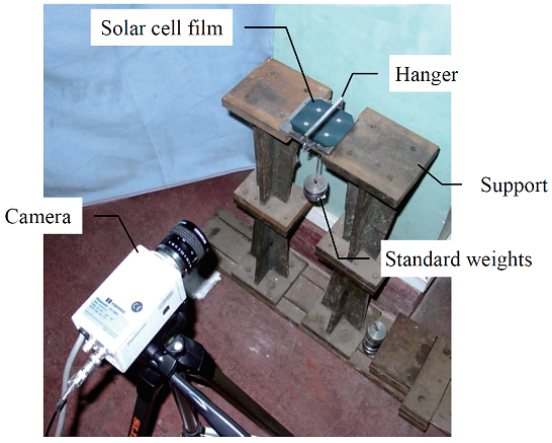


Fig. 6 Experimental system for measuring the solar cell film stiffness

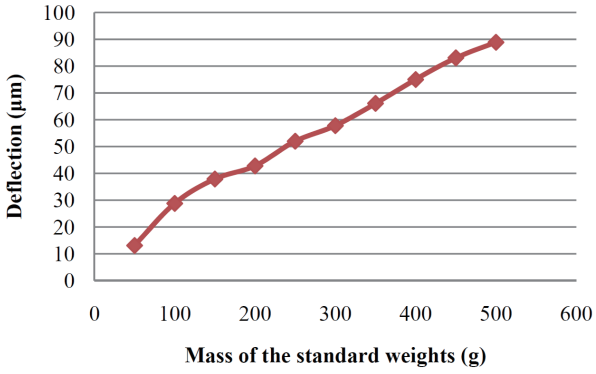


Fig. 7 Load-deflection curve of a solar cell film

https://doi.org/10.1017/jmech.2014.5 Published online by Cambridge University Press

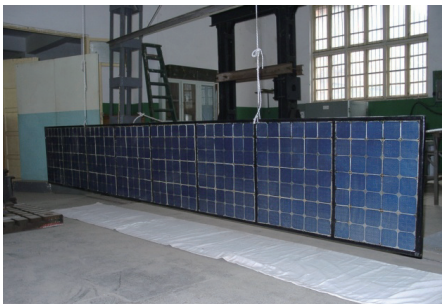
Table 1 Comparison of the first five natural frequencies of a LSSAS

Mode No.	Simulation results using the proposed model	Simulation results by ANSYS software	Results by modal analysis experiment	Relative error (%)
1	4.311	4.323	4.30	0.26
2	9.165	9.187	8.94	2.52
3	11.874	11.989	12.21	2.75
4	15.583	15.612	16.02	2.73
5	19.251	19.874	19.82	2.87

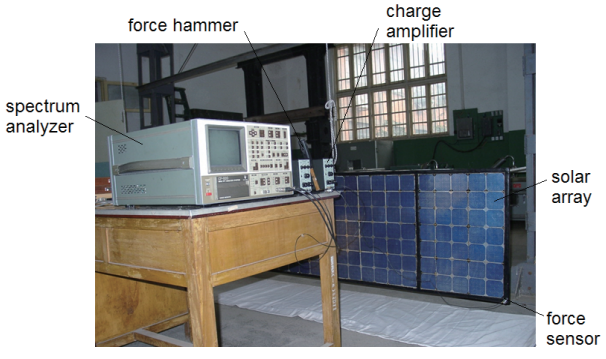
3.2 Solar Array Modal Analysis Experiment

Now we conduct a modal analysis experiment to verify the accurateness of the proposed model. As shown in Fig. 8(a), an experimental model of a large semi-rigid solar array structure with dimensions of 4800 × 600 × 15mm is designed. Then, a modal analysis experimental system for testing the modal frequencies of the designed solar array structure is established. The composition of this modal experimental system is illustrated in Fig. 8(b).

The experimental results of the first five frequencies of this semi-rigid solar array structure are listed in Table 1. By comparing to the results by the proposed membrane-frame model, it can be observed that these natural frequencies are showing good consistence with each other (the maximum relative error is less than 3%). Thus, the correctness of the proposed model has been demonstrated.



(a) Tested object of a solar array structure



(b) Diagram of modal experiment equipments

Fig. 8 Modal analysis experiment system for a large semi-rigid solar array

4. CONCLUSIONS

LSSAS is very promising for the large power devices of many spacecraft such as of spaceships, space stations and space laboratories. To solve complex dynamic problem encountered in the design and control of such semi-rigid structure, an innovative analytical dynamic model for analyzing its dynamic characteristics is developed in this paper. Furthermore, efficient experimental method is proposed for measuring the dynamic parameters of this special kind of rigid-flexible coupling structure. From the present paper, we can conclude that:

1. The presented dynamic model, namely membrane-frame model, has provided a novel idea for solving the dynamic modeling problem of this typical kind of semi-rigid space structure.
2. The proposed experimental method has given feasible and effective approach to measure the dynamic parameters of this complex rigid-flexible coupling structure.
3. Through the way of numerical simulation and experimental research, the presented analytical dynamic modeling method is verified to be accurate and valid.
4. Based on the dynamic modeling and experiment method proposed in this paper, we can acquire the dynamic characteristics of this kind of large semi-rigid structure. The research results in this paper are very valuable for the structural design and control system design of this structure in the engineering. As a subsequent extension of this study, shape maintaining and vibration control of such semi-rigid structure need further investigations.

ACKNOWLEDGEMENTS

The authors would like to appreciate the financial support from the National High-tech Research and Development Program of China and the National Natural Science Foundation of China.

REFERENCES

1. Pai, P. F. and Young, L. G., "Modeling, Analysis and Testing of Some Deployable/Inflatable Structures," *Proceedings of 45th AIAA/ASME/ASCE/AHS/ASC Structures, Structural Dynamics and Materials Conference*, Palm Springs, California, USA (2004).
2. Foster, J. A. and Aglietti, G. S., "The Thermal Environment Encountered in Space by a Multifunctional Solar Array," *Aerospace Science and Technology*, **14**, pp. 213–219 (2010).
3. Lore, K. F. and Smith, S. W., "Efficient Computation of Dynamic Response of Large Flexible Spacecraft," *Proceedings of 46th AIAA/ASME/ASCE/AHS/ASC Structures, Structural Dynamics and Materials Conference*, Austin, Texas, USA (2005).

https://doi.org/10.1017/jmech.2014.5 Published online by Cambridge University Press

4. Chang, T.-P., "Stochastic Dynamic Response of a Simplified Nonlinear Fluid Model for Viscoelastic Materials," *Journal of Mechanics*, **28**, pp. 365–372 (2012).
5. Smith, S. W. and Mei, K., "Analytical Models for Nonlinear Response of a Laboratory Solar Array," *Proceedings of 38th AIAA/ASME/ASCE/AHS/ASC Structures, Structural Dynamics, and Materials Conference*, Kissimmee, Florida, USA, pp. 809–819 (1997).
6. Ko, K.-E. and Kim, J.-H., "Thermally Induced Vibrations of Spinning Thin-Walled Composite Beam," *AIAA Journal*, **41**, pp. 296–303 (2003).
7. Carney, K. S. and Shaker, F. J., "Free-Vibration Characteristics and Correlation of a Space Station Split-Blanket Solar Array," *Proceedings of 30th AIAA/ASME/ASCE/AHS/ASC Structures, Structural Dynamics, and Materials Conference*, Mobile, Alabama, USA, pp. 812–819 (1989).
8. Mockensturm, E. M., Pappa, R. S., Woods-Vedeler, J. A. and O'Neill, M. J., "Static and Dynamic Analysis of Stretched Membrane Lenses for Lightweight Space Solar Arrays," *Proceedings of 3rd AIAA Gossamer Spacecraft Forum*, Denver, Colorado, USA (2002).
9. Sowmianarayanan, S. and Pradeept, S., "Vibration Suppression of a Spacecraft Solar Array Using On-Off Thrusters," *Proceedings of 40th AIAA/ASME/ASCE/AHS/ASC Structures, Structural Dynamics, and Materials Conference and Exhibit*, St. Louis, Missouri, USA, pp. 3097–3106 (1999).
10. Pai, P. F. and Schulz, M. J., "Modeling of Highly Flexible Structures," *Journal of Spacecraft and Rockets*, **37**, pp. 419–421 (2000).
11. Morozov, E. V. and Lopatin, A. V., "Design and Analysis of the Composite Lattice Frame of a Spacecraft Solar Array," *Composite Structures*, **93**, pp. 1640–1648 (2011).
12. Zajkani, A., Shirkoohi, H. S., Darvizeh, A., Darvizeh, M. and Babaei, H. G., "Mathematical Modeling of Large-Amplitude Dynamic-Plastic Behavior of Circular Plates Subjected to Impulsive Loads," *Journal of Mechanics*, **26**, pp. 533–546 (2010).
13. Wua, J., Yan, S. and Xie, L., "Reliability Analysis Method of a Solar Array by Using Fault Tree Analysis and Fuzzy Reasoning Petri Net," *Acta Astronautica*, **69**, pp. 960–968 (2011).
14. DFH-3. Http://www.astronautix.com/craft/dfh3.htm.
15. Inman, D. J., *Vibration and Control*, 1st Edition, John Wiley & Sons, Chichester, West Sussex, England, pp. 264–268 (2006).
16. Wie, B., *Space Vehicle Dynamics and Control*, 2nd Edition, AIAA, Reston, Virginia, USA, pp. 485–491 (2008).
17. Gere, J. M. and Goodno, B. J., *Mechanics of Materials*, 8th Edition, Cengage Learning, Stamford, Connecticut, USA, pp. 756–771 (2012).

(Manuscript received November 21, 2012,
accepted for publication August 27, 2013.)

https://doi.org/10.1017/jmech.2014.5 Published online by Cambridge University Press